



## MAGIC measurement of the Crab Nebula spectrum over three decades in energy

ZANIN, R.<sup>1</sup>, MAZIN, D.<sup>1</sup>, CARMONA, E.<sup>2</sup>, COLIN, P.<sup>3</sup>, CORTINA, J.<sup>1</sup>, JOGLER, T.<sup>3</sup>, KLEPSEK, S.<sup>1</sup>, MORALEJO, A.<sup>1</sup>, SITAREK J.<sup>4</sup>, FOR THE MAGIC COLLABORATION, AND HORNS, D.<sup>5</sup> AND MEYER M.<sup>5</sup>

<sup>1</sup>*Intitut de Fisica d'Altes Energies, Bellaterra, Spain*

<sup>2</sup>*Centro de Investigaciones Energéticas, Medioambientales y Tecnológicas, Madrid, Spain*

<sup>3</sup>*Max-Planck Institut, Munich, Germany*

<sup>4</sup>*University of Łódź, Poland*

<sup>5</sup>*University of Hamburg, Germany*

roberta@ifae.es

**Abstract:** The Crab Pulsar Wind Nebula is the best studied source of  $\gamma$ -ray astrophysics. The contribution of the various soft radiation fields to the Inverse Compton component of its high energy emission, the strenght of the internal magnetic field and the maximum energies reached by primary electrons are however still matter of study.

The MAGIC stereoscopic system recorded almost 50 hours of Crab Nebula data in the last two years, between October 2009 and April 2011. Analysis of this data sample using the latest improvements in the MAGIC stereo software provided an unprecedented differential energy spectrum spanning three decades in energy, from 50 GeV up to 45 TeV. At low energies, the MAGIC results, combined with the Fermi/LAT data, yield a precise measurement of the Inverse Compton peak. In addition, we present light curves of the Crab Nebula at different time scales, including a measurement simultaneous to one of the Crab Nebula flares recently detected by both Fermi/LAT and AGILE. Using the MAGIC spectrum together with multiwavelength data, we discuss the implications for the modeling of the Crab Nebula.

**Keywords:** Crab Nebula, Pulsar Wind Nebulae, MAGIC telescopes, Cherenkov, very high energy

## 1 Introduction

The pulsar wind nebula (PWN) associated with the Crab Pulsar is a leftover of a supernova explosion recorded in 1054 [1]. Located at the center of the nebula, the pulsar continuously releases its energy primarily in the form of a highly relativistic and magnetized wind of particles, mainly electrons and positrons. This pulsar wind terminates in a standing shock where particles are accelerated up to ultra-relativistic energies, and their pitch angles are randomized. The outflow interacts with the surrounding magnetic and photon fields creating the PWN. The nebula emits synchrotron radiation which is observed from radio frequencies up to soft  $\gamma$ -rays. This emission is well-described in terms of the magnetohydrodynamic model (MHD) [2]. At higher energies (above 500 MeV), the overall emission is dominated by the Inverse Compton (IC) scattering by the electrons from the pulsar, predominantly on the synchrotron photons [3].

The Crab Nebula is one of the best-studied non-stellar objects in the sky. Due to its bright glow at almost all wavelengths, precise measurements can be provided by many different kinds of instruments, allowing for a detailed examination of its physics.

The IC emission from the Crab Nebula was detected for

the first time above 700 GeV by the pioneering Whipple telescope in 1989 [4]. Since then, the imaging Cherenkov technique was successfully used to extend the Crab Nebula differential energy spectrum from a hundred GeV up to a hundred TeV. Nevertheless, the low-energy part of this component, below 100 GeV, where the IC peak resides, could be observed only in the last years. At low energies, the *Fermi* satellite filled the gap between few and hundred GeV [5]. In the meanwhile, the construction of imaging atmospheric Cherenkov telescopes (IACTs) with larger reflective surface allowed to lower the energy threshold of the ground-based telescopes below 100 GeV. The stand-alone first MAGIC telescope had already shown a hardening of the spectrum below a few hundreds GeV [6]. With an energy threshold of 80 GeV, MAGIC provided the only experimental data points overlapping with the *Fermi*/LAT ones up to now. The goal of this work is to measure the Crab Nebula differential energy spectrum with a higher statistical precision and down to lowest possible energy threshold by using the MAGIC stereoscopic system.

In addition, because of its apparent overall flux steadiness, the Crab Nebula has been considered as standard candle at almost all wavelengths. It has been used to cross-calibrate X-ray and  $\gamma$ -ray telescopes, to check the instrument performance over time, and to provide units for the emission of

other astrophysical objects. However, this notion surprisingly changed in September 2010, when both *AGILE* and *Fermi/LAT* satellites observed an enhancement of the  $\gamma$ -ray flux above 100 MeV by a factor 2 [7, 8]. Spectral analysis revealed that the flare had a synchrotron origin, and a spectrum which is harder than the average one. Optical and X-ray images taken right after the flare showed a few nebular, brightened features. One of them is the “anvil”, the knot which lies in the inner nebula in the projected inward extension of the jet, and it is considered a primary site for particle acceleration. If the  $\gamma$ -ray flare luminosity suggests that the production region is close to the pulsar, the short flare rising time favors a compact emission region of size smaller than  $10^{16}$  cm. Thus, the “anvil” feature could be an excellent flare site candidate [7]. A similar episode was observed in April 2011 by the same teams (ATel #3276). It lasted for two weeks, with the peak occurring on April 14, 2011.

The MAGIC telescopes recorded some data simultaneously to both high-energy  $\gamma$ -ray flares in September 2010 and April 2011. The results of these observations will also be presented in this paper.

## 2 The MAGIC telescopes

MAGIC consists of two 17 m diameter IACTs located in the Canary island of La Palma, Spain (2200 m above sea level). It became a stereoscopic system in Autumn 2009. The stereoscopic observation mode led to a significant improvement in the performance of the instrument [9][10]. The current sensitivity of the array yields  $5\sigma$  significance detections above 250 GeV of fluxes as low as 0.8% of the Crab Nebula flux in 50 hr. The energy threshold of the analysis lowered down to 50 GeV for low zenith angle observations.

For this work we considered stereoscopic observations of the Crab Nebula carried out during the last two years, between October 2009 and March 2011. These observations are performed in wobble mode, at zenith angles between  $5^\circ$  and  $50^\circ$ . Data affected by hardware problems, bad atmospheric conditions, or displaying unusual background rates were rejected in order to ensure a stable performance. 48.7 hours of effective time are left after data quality selection.

The analysis was performed by using the tools of the MAGIC analysis software [11]. Each telescope records only the events selected by the hardware stereo trigger. The so-called image cleaning procedure selects the pixels which have significant signal. The obtained reconstructed image is then parametrized with a few simple quantities. In particular, we use a new algorithm, the so-called *sum image cleaning* to improve the analysis sensitivity at energies below 100 GeV. Similarly to the standard algorithm it uses the concept of core and boundary pixels, defined according to their charge levels. The addition of new constraints on the charge level of compact group of neighboring core pixels, within a very short time spread, further allows to lower the charge thresholds. This is an important aspect in the

reconstruction of low-energy shower images which contain only few pixels. The *sum image cleaning* performs as well as the standard one for energies above 150 GeV, whereas below such energies it improves the sensitivity by a 15%.

Afterwards, pairs of images from the same stereo events are combined and the shower direction is determined as the average of the corresponding single-telescope directions [10]. The background rejection relies on the definition of the multi-variable variable *hadronness*, which is computed by means of a Random Forest (RF) algorithm. RF uses as input a small set of image parameters from both telescopes, together with the information about the shower location provided by stereoscopy. The  $\gamma$ -ray signal is estimated through the distribution of the squared angular distance ( $\theta^2$ ) between the reconstructed and the catalog source position. The energy of each event is estimated by using look-up tables created from Monte Carlo simulated  $\gamma$ -ray events. For the computation of the differential energy spectrum, the  $\gamma$ -ray signals in each energy bin are determined by selecting a soft *hadronness* cut which retains 90% of the  $\gamma$ -ray events.

The data sample was divided in four zenith angle ranges to account for corresponding variations in the image parameters. The matrices for the background rejection obtained through the RF were computed for each sub-sample separately. The four independent analyses were combined later at the last stage of the analysis. In Figure 1 we show the collection area obtained for the four data sub-samples.

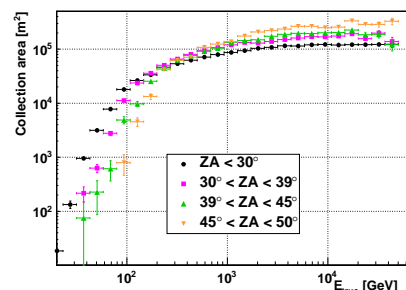


Figure 1: Collection area obtained for the data sub-samples in the four different ranges of zenith angle.

## 3 The differential energy spectrum

Figure 2 shows an unprecedented differential energy spectrum of the Crab Nebula which spans three orders of magnitude in energy, from 50 GeV up to 45 TeV. In order to correct for the finite energy resolution and energy estimation bias it was unfolded with Bertero’s method [13]. Three other unfolding methods were considered, and all of them gave compatible results within the statistical errors. The yellow-shadowed area indicates the systematic uncertainties on the flux normalization and the spectral slope. The first one is estimated to be 15% of the flux value, whereas the second one produces an absolute uncertainty on the

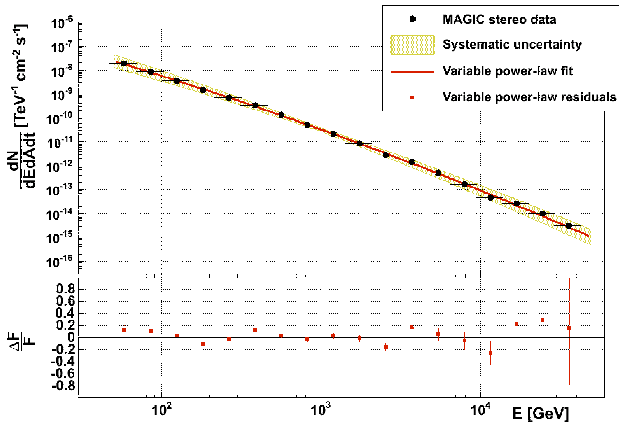


Figure 2: Differential energy spectrum of the Crab Nebula obtained with data recorded by the MAGIC stereoscopic system.

photon index of 0.15. Additionally, there is another systematic uncertainty affecting the energy scale measurement at the level of 15–17%. Systematic uncertainties, related to the non-perfect matching of the observation conditions and the Monte Carlo simulations, have been estimated by studying the spectra reconstructed in different zenith angle ranges, analysis cuts, mis-pointing values, night sky background levels [10]. At all energies, the overall uncertainty is dominated by systematic errors rather than statistical ones. We fit the differential spectrum with a variable power-law:

$$\frac{dN}{dE dt dA} = f_0 \left( \frac{E}{1 \text{ TeV}} \right)^{-\alpha + b \cdot \text{Log}_{10} \left( \frac{E}{1 \text{ TeV}} \right)} \frac{\text{photons}}{\text{TeV cm}^2 \text{ s}} \quad (1)$$

where  $f_0 = (3.27 \pm 0.03_{stat}) \times 10^{-11}$ ,  $\alpha = 2.40 \pm 0.01_{stat}$ , and  $b = -0.15 \pm 0.01_{stat}$ . The residuals to the fit show significant deviations which are explained by systematic effects ( $\chi^2/ndf = 72/15$ ).

Figure 3 shows the spectral energy distribution (SED) for the same data points in Figure 2, and compares it to other measurements by IACTs. At energies above 10 TeV, given the large systematic error, it is not possible to disentangle the discrepancies between the results obtained by HESS [15] and those by HEGRA [14].

In order to estimate the position of the IC peak we fit a variable power-law function to our data combined with the *Fermi*/LAT data points taken from [5]. The fit accounts for the correlation in MAGIC data point and considers statistical errors only. The obtained IC peak is  $59 \pm 6$  GeV.

## 4 The light curve

In this section we present a time-resolved measurement, i.e. the light curve, of the  $\gamma$ -ray flux above 300 GeV from the Crab Nebula. This is meant to check the flux stability on timescales of days. Results are shown in Figure 4. The upper panel shows the light curve between October 1,

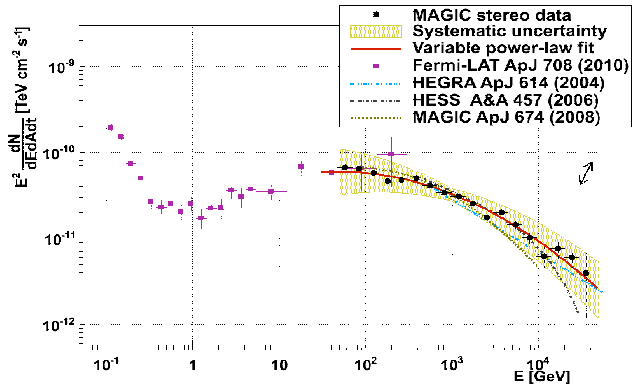


Figure 3: Spectral energy distribution of the Crab Nebula obtained with the MAGIC telescopes, together with the results from previous  $\gamma$ -ray experiments. The black arrow indicates the systematic uncertainty on the energy scale.

2009 and March 31, 2011. In addition, the bottom panels are zoomed per-month portions of the bottom panel. The average flux of all nights  $F_{>300 \text{ GeV}}$  is:

$$F_{>300 \text{ GeV}} = (1.31 \pm 0.03_{stat} \pm 0.17_{sys}) \times 10^{-10} \text{ cm}^{-2} \text{ s}^{-1}. \quad (2)$$

The Crab Nebula flux is stable within the systematic uncertainty with a probability of 95%. The red shadow area in the panel marks the period of the enhanced  $\gamma$ -ray flux detected by both *AGILE* and *Fermi* in September 2010. MAGIC observed the Crab Nebula for one night during the same period, on September 20, 2010. The obtained flux is perfectly compatible with the average flux of all the nights within the statistical error.

In addition to the sample used for the analysis presented up to here, we took some data between April 12 and 14, 2011, for a total amount of about 140 minutes. These observations were carried out under strong moonlight conditions with a special high voltage setting. A preliminary analysis of this second data set shows no increase in flux, as illustrated in Figure 5.

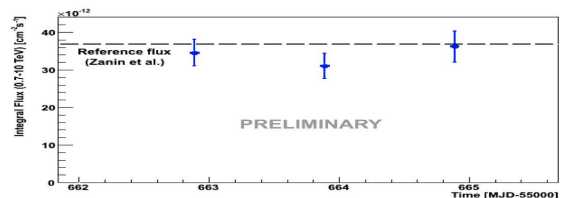


Figure 5: Light curve of the Crab Nebula between April, 12 and 14 during the flare detected at high-energies.

## 5 Discussion

The broad-band SED of the Crab Nebula has been matched with two different model calculations that are based on the model first suggested by [16] assuming a constant magnetic

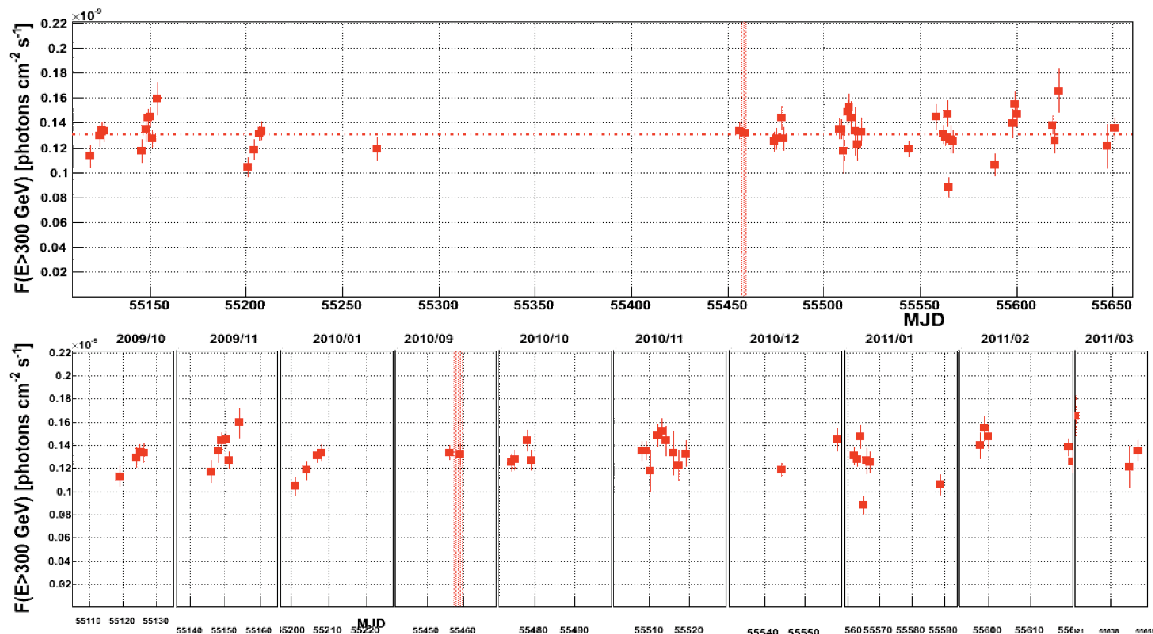


Figure 4: Light curve of the Crab Nebula.

field,  $B$ , as well as a solution of the ideal radial MHD flow [2]. The best match of the free model parameters (average B-field and magnetization of the flow at the shock,  $\sigma$ ) to the measured SED has been obtained using a rather weak field of  $B = (124 \pm 6) \mu G$  [17] or a value  $\sigma = 0.0045 \pm 0.0003$ . Both model calculations are shown in Figure 6 together with the archival data as well as the new measurement presented here. The spectral measurement obtained with the MAGIC telescopes covers for the first time the crucial energy range at the peak of the IC component. None of the models provide a satisfactory match to the data if we consider statistical errors only. However, if taking systematic uncertainties into account, both models can fit the observations. In case the systematic errors of the measurement can be further reduced, the new measurement can therefore help to lift a degeneracy and will require the introduction of additional structure in the B-field downstream of the shock. Specifically, the shape of the spectrum at  $\approx 100$  GeV which is sensitive to the B-field in the region well outside the torus of the Crab Nebula.

The constant B-field model offers the opportunity to cross calibrate the IACT measurements with *Fermi*/LAT observations. For the IACTs an energy scaling factor  $s_{\text{IACT}}$  is introduced to correct the measured energy  $E_{\text{meas}}$  to a common energy scale  $E = s_{\text{IACT}} \times E_{\text{meas}}$ . This procedure reduces the uncertainty of the energy scale to that of the *Fermi*/LAT [17]. The scaling factor is determined via a  $\chi^2$ -minimization and is found to be  $s_{\text{IACT}} = 1.050 \pm 0.003$ .

## References

[1] Stephenson, F.R., Green, D.A., International series in astronomy and astrophysics, 2002, **5**

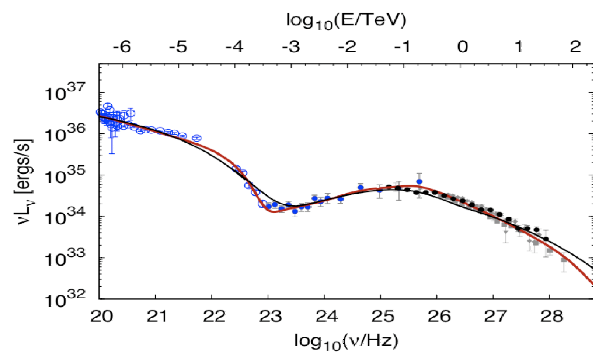


Figure 6: Measurements of the Crab Nebula SED (filled black circles are MAGIC data presented here and filled blue circles *Fermi*/LAT points) overlaid to two different models: the constant B-field (red line) and the MHD (black line).

- [2] Kennel, Coroniti, ApJ, 1984, **283**: 710
- [3] Atoyan, A.M., Aharonian, F., MNRAS, 1996, **278**: 525
- [4] Weekes, T. et al., ApJ, 1989, **342**:379
- [5] Abdo, A. et al., ApJ, 2010, **708**:1254
- [6] Albert, J. et al., ApJ, 2008, **674**:1037
- [7] Tavani, M. et al, Science, 2011, **331**: 736
- [8] Abdo, A. et al., Science, 2011, **331**: 739
- [9] Carmona, E. et al., These proceedings.
- [10] Aleksić, J. et al., submitted to Astroparticle Journal
- [11] Lombardi, S. et al., These proceedings.
- [12] Aleksić, J. et al., A&A, 2010, **524**: A77
- [13] Bertero, M., Advances in electronics and electrons physics, p.120.
- [14] Aharonian, F. et al., ApJ, 2004, **614**: 847
- [15] Aharonian F. et al., A&A, 2006, **457**: 899
- [16] Hillas et al., ApJ, 1998, **503**: 744
- [17] Meyer M. et al., A&A, 2010, **523**: A2